MECHANIKA TEORETYCZNA
I STOSOWANA
Journal of Theoretical
and Applied Mechanics
3, 33, 1995

MICROSTRUCTURAL EFFECT ON FRACTURE TOUGHNESS OF N26MT2Nb STEEL IN THE TWO-PHASE STATE

JERZY JELEŃKOWSKI

Department of Materials Science and Engineering

Warsaw University of Technology

The aim of investigation was to determine the effect of the Ni26MoTi2Nb alloy (C – 0.02%, Ni – 26.0%, Ti – 2.15%, Mo – 1.15%, Nb – 0.11%) tempering for 40 minutes in the temperature range $A_s \div A_f$[1]; i.e., within the transformation range of martensite (α') into austenite (γ), on its microstructure and fracture toughness. The initial structure of alloy was composed of martensite ($\sim 70\%$) and retained austenite $\sim 30\%$). During tempering, the alloy underwent ageing. The highest values of fracture toughness J_{Ic}, four times higher than those in the initial state, were achieved after tempering at 975 K; i.e., at a temperature close to A_f. At this tempering temperature, the austenite content doubled while the tensile strength increased more than threefold. An increase in the martensite content, found on fracture surfaces of specimens held at the upper temperature zone of the $\alpha' \rightarrow \gamma$ transformation, amounting to $10 \div 15\%$ as compared with the undeformed region, proves the metastability of reverted austenite[2] and beneficial results of the transformation into martensite during deformation.

1. Introduction

The Ni26MoTi2Nb alloy belongs to the group of transition alloys in which, depending on the heat treatment conditions applied, an austenitic

[1]The reverse transformation of martensite into austenite ($\alpha' \rightarrow \gamma$) is characterized by the A_s (start) and A_f (end) temperatures (where $A_s < A_f$). The end (A_f) of the martensite-to-austenite reaction on heating may occur at a temperature at which the austenite is not stable relative to other phases in the equilibrium diagram.

[2]Reverted austenite – the austenite formed by the reverse transformation.

or austenitic-martensitic structure is obtained (cf Verhoeven (1975); Kokorin (1987); Gorbach et al. (1989); Sagaradze and Uvarov (1989)). The M_s[3] temperature of this alloys lies below 273 K while its M_f temperature is inferior to 77 K (cf Kordonskiy (1974); Jeleńkowski and Filipiuk (1991)). For this reason, a considerable amount of retained austenite subsists even after low-temperature treatments in liquid nitrogen. The temperatures M_s and M_f can be markedly raised by destabilization of the austenite, but the wholly martensitic structure is from the economical point of view not desired.

Austenitic and martensitic-austenitic alloys are applied in the strengthened conditions provided by ageing or phase hardening. A microstructure is now being sought which could ensure a high fracture toughness, as this property is of paramount importance as regards the application of high-strength constructional alloys.

Mechanical properties of the Ni26MoTi2Nb alloy after some selected heat treatment processes are given in Table 1 (cf Jeleńkowski and Filipiuk (1991)).

Table 1

	R_m [MPa]	$R_{0.2}$ [MPa]	A_{10} [%]	J_{Ic} [kJ/m^2]
In the austenitic homogenized conditions*	575	190	46	15
After austenitizing at 1223 K for 2 hours and cold treatment for 0.5 hour in liquid nitrogen	935	480	15	18
After quench hardening as above, reaustenitizing at 1000 K and cooling in air	1355	725	12	25
After quench hardening as above and ageing for 2 h at 1000 K	1375	605	9	20

* The grain size corresponds to No.6 after the ASTM scale.

Similar values of tensile properties and fracture toughness can be obtained for many cheaper alloys and under more economical heat treatment conditions than the aforementioned ones.

As earlier investigations have trough into light (cf Jeleńkowski and Filipiuk (1991)), the retained austenite in the Ni26MoTi2Nb alloy can exhibit meta-

[3] M_s – temperature at which the undercooled austenite starts to transform into martensite. M_f – temperature at which the transformation of undercooled austenite into martensite – during continuous cooling – ends.

stability; i.e., the ability to be transformed into martensite during deformation (TRIP – Transformation Induced Plasticity – effect (cf Zackay et al. (1967); Gerberich et al. (1968)). It has been found that the reverted austenite which forms in the reverse transformation, can also be metastable.

In an alloy with metastable austenite an additional marked contribution to strengthening originates from the deformation due to the martensitic transformation. This phenomenon can afect an abrupt change not only in the chemical and physical properties, but also in the tensile strength, fracture toughness, fatigue strength and wear resistance, respectively. Percentage elongation and fracture toughness can be here markedly multiplied by the TRIP effect (cf Schmidt (1989)). If the chemical composition and heat treatment conditions enable a considerable amount of metastable austenite to be left in the structure, a material with a tensile strength of up to 2000 MPa and elongation of up to 25% can be obtained (cf Zackay et al. (1967)). However some side-effects of the metastability of austenite, which manifest themselves by a localization of plastic deformation and by brittleness, can appear. This markedly decreases the interest in these alloys. In the author's opinion, the structural reasons for the appearance of such disadvantageous characteristics of the alloys are to be sought in the mechanisms of the martensitic transformation induced by deformation (cf Olson et al. (1987); Schmidt (1989)).

The martensitic transformation can take place spontaneously on passing through the M_s temperature or through the A_s temperature in reverse transformation; i.e., transformation of martensite into austenite (Fig.1, cf Hornbogrn (1984)). Austenite can transform into martensite if a shear stress τ_{am} is applied in the direction of the martensitic shear which would have occured below M_s in the absence of external forces. The value of τ_{am} is zero at the martensitic start temperature M_s and increases with decreasing undercooling $\Delta T < T_0 - M_s$; i.e., with the decreasing value of chemical driving force for the martensitic transformation as illustrated in Fig.1. During deformation in the temperature range $M_s - M_d$ the deformation induced transformation occurs in deformed regions and is most clearly visible at the intersection of slip bands. Above the M_d temperature, a deformation induced martensitic transformation is not feasible. The equlilibrium temperature T_0 which plays in the martensitic transformation an essential role, depends on the chemical composition of the alloy, degree of order of the parent phase and value of hydrostatic stress. Undercooling ΔT which also constitutes an important factor, is influenced by the martensite nucleation and growth conditions inside the matrix which, in turn, depend on the value of shear stress τ_a and the strength of the parent phase (cf Hornbogrn (1984); Schmidt (1989)).

It is an easier task to follow changes in the values of critical temperatures

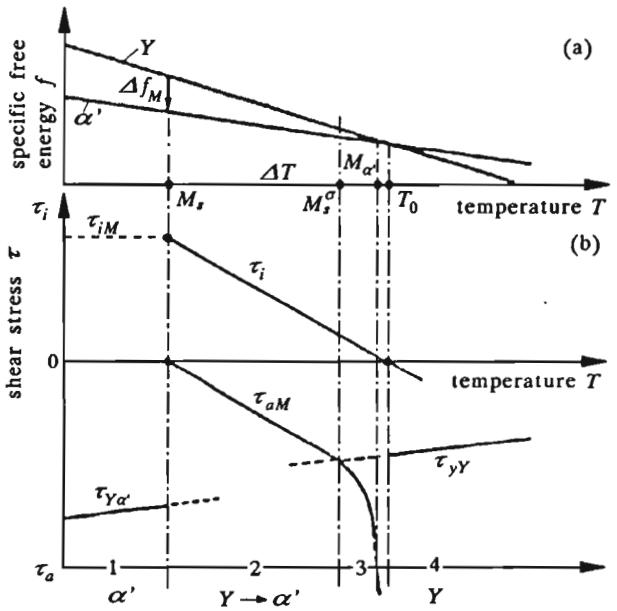

Fig. 1. Schematic representation of thermodynamic and mechanical properties of undercooled austenite (γ): (a) – free energy of the phase γ and martensite (α') versus temperature, (b) — at $T < T_0$ the mean internal shear stress τ_i increases and induces a spontaneous transformation at $\tau_i = \tau_{im}$. With decreasing ΔT the external shear stress τ_{am} necessary to cause transformation is partially reduced by the increasing shear stress τ_i. τ_{im} becomes zero at the M_s temperature. $\tau_{y\alpha}$ and $\tau_{y\gamma}$ denote the yield points in shearing of martensite and austenite, respectively (cf Hornbogrn (1984)) (with commented by author). Range 1: $\gamma\alpha'$ transformation occurs on cooling. External shear stress is not necessary. Range 2: $\gamma\alpha'$ transformation is induced by stress. Range 3: Deformed metastable austenite transforms into strain-induced martensite (strain-induced $\gamma\alpha'$ transformation). Range 4: Austenite is stable, no martensite is formed.

and in the transformation kinetics than to observe subtle variations in the chemical composition within microregions, in the degree of order of the parent phase and in the value of coherent stresses which determine the site and mode of nucleation of the martensitic phase.

The lack of success experienced by researchers (cf Decker (1963); Kordonskiy (1974); Pickering (1978)) in developing steels with ~25%Ni has for a long time hampered their evolution, but at the same time, contributed to the appearance of maraging steels whichhave become well known now. Less expensive alloys with the properties comparable to these of maraging steels, are still being sought after. These requirements seem to be fulfilled by the Fe-Ni-T-Mo alloys containing $25 \div 28$%Ni, ~ 2%Ti and ~1%Mo. One to a high content

of Ni, the martensitic transformation can occur even at a slow cooling rate. Ti, Al, Mo and Nb are responsible for strengthening with the participation of the reverse transformation. The present work presents an attempt to find an alloy with metastable reverted austenite, characterized by a high strength and good fracture toughness.

2. Reverse transformation in Fe-(20-32)Ni-base alloys

The reverse transformation in Fe-Ni-base alloys still demands satisfactory explanation (cf Malyshev et al. (1982); Kokorin (1987); Gorbach et al. (1989); Sagaradze and Uvarov (1989)). The most controversial is the view on the change of the diffusional kinetics into a diffusionless one, taking place with a change in temperature, as well as the effect of temperature on the transformation. The mechanism of the transformation depends, as it has been proved (cf Jana and Wayman (1967); Kessler and Pitsch (1967); Davies and Magee (1970) and (1971); Kulinchev and Perkas (1970); Richman and Bolling (1971)), on the heating rate and its complexity may be attributed to the processes of dissolution and precipitation of intermetallic phases as well as to the redistribution of nickel between martensite and austenite. According to works by Jana and Wayman (1967), Kessler and Pitsch (1967), Davies and Magee (1970), there exists a critical value of the heating rate above which diffusional processes are stopped and the A_f temperature remains constant. At slow heating rates a complicated relationship between the content of reverted austenite and temperature was observed. This was earlier explained (cf Jana and Wayman (1967); Kessler and Pitsch (1967); Davies and Magee (1970) and (1971)) to be a result of alternation between different mechanisms of transformation. The transformation is most often slowed down after start whereupon it becomes intensified and, at the final stage, stopped. The initial phase extends with a decrease in tempering temperature. Thermokinetic curves of the reverse transformation in alloys subjected previously to ageing show a similar course, but their beginnings are shifted towards higer temperatures. The impoverishment of austenite in elements which have entered into the precipitates, is probably responsible for the transformation shift. For this reason, in previously aged specimens a smaller proportion of reverted austenite occurs than in those subjected only to the quench hardening (cf Kordonskiy (1974); Dekhtyar et al. (1984); Gorbach et al. (1984) and (1986)).

When investigating of the reverse transformation in alloys with a chemical composition approximating that of the steel involved, the probability of occur-

rence of ferromagnetic austenite and of the phenomenon of invar strengthening was analysed (cf Kulinchev and Perkas (1970); Davies and Magee (1971); Richman and Bolling (1971); Dekhtyar (1984)). It has been found that in alloys of the Fe-(27-29)-2Ti or Fe-(24-28)Ni type, the ferromagnetic austenite did not occur while the reverted austenite showed a tendency to metastability, not observed in the invar (cf Kordonskiy (1974); Dekhtyar et al. (1984); Gorbach et al. (1984) and (1986); Kokorin (1987); Sagaradze and Uvarov (1989)).

One can assume that the metastability of austenite depends on the mechanism of reverse transformation and that it is more easily accomplished in alloys which do not show the tendency to invar strengthening. This creates the possibility of control the metastability of reverted austenite in these alloys and raises hopes of achieving a progress in developing Fe-25Ni base alloys with high tensile strength and good fracture toughness. To make a contribution to the investigation of this problem is the aim of the present work.

3. Material for investigation, heat treatment applied and methods of investigation

The investigations were conducted on specimens of Ni26MoTi2Nb steel of the composition given below in percentage by weight, originating from an experimental melt:

C	–	0.02	Ni	–	26.0
Mn	–	0.17	Ti	–	2.15
Si	–	0.11	Mo	–	1.15
P	–	0.007	Nb	–	0.11
S	–	0.009	Al	–	0.04

3.1. Heat treatment

All specimens to be investigated were homogenized for 8 hours at 1373 K, austenitized at 1223 K (heating and tempering was carried out in a vacuum furnace at the pressure of ~1 daPa) and then quenched in water and cold treated for 0.5 hour in liquid nitrogen. The quench-hardened specimens contained ~70% of martensite. The $\alpha' \rightarrow \gamma$ transformation was realized by heating at a rate of 5 K/min and tempering for 40 minutes at 925, 950, 975, 1000 and 1025 K, respectively; i.e., at temperatures within the $\alpha' \rightarrow \gamma$ transformation

range established by means of the dilatometric and calorimetric analysis. After tempering at the temperature desired, the specimens were cooled in water.

3.2. Experimental procedure

In the calorimetric and dilatometric analysis, the critical temperatures of the $\alpha' \rightarrow \gamma$ transformation as well as the temperature ranges of the accompanying processes were established. For calorimetric analysis purposes the scanning differential Perkin-Elmer DSC-2 calorimeter with a measuring range 293÷999.9 K was used. A constant heating rate of 30 K/min was applied while the cooling rate was equal to 320 K/min. The dilatometric curves were recorded using a Chevenard dilatometer. In the dilatometric analysis the specimens were heated at a constant rate of 5 K/min up to 1100 K and cooled down first to ~500 K in the air-blast dilatometer furnace and then, to room temperature, in air.

Metallographic examinations were carried out on specimens prepared by standard techniques and etched with nital. Etched microsections were subjected to microhardness measurements by the Vickers method upon a load of 100 g.

The proportion of martensite in the microstructure was determined by the X-ray and magnetometric method.

The microstructure of thin foils was observed on the JEOL 100B transmission microscope at an accelerating voltage of 100 kV.

Fraction toughness tests were performed by the J integral method on a MTS machine using specimens of the CT(D) type (24 mm in diameter, 6 mm thick and 18 mm wide), in accordance with the requirements of the ASTM E813-82 standard. The tensile test was carried out on specimens of 5 mm in diameter with a gauge lenth of 50 mm. For the examination of fracture surfaces a Tesla scanning microscope was used.

4. Results of experiments

4.1. Dilatometric and calorimetric analysis

From the dilatometric curve (Fig.2) the critical temperatures of the $\alpha' \rightarrow \gamma$ transformation, namely A_s and A_f, were determined. The transformation starts at ~760 K and finishes at ~1030 K. The curve shows the stages of

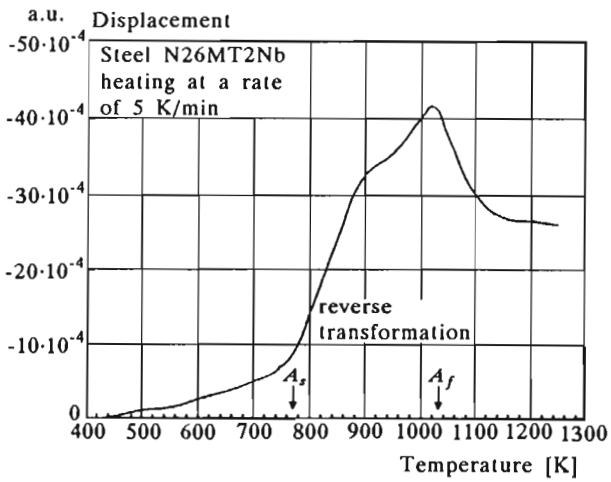

Fig. 2. Dilatometric curve of the reverse transformation with the critical temperatures marked therein

reverse transformation; namely, the initial moderate course until ~840 K, slowing-down in the temperature range 840÷925 K, fast course in the range 925÷965 K and final slowing-down above 970 K.

From the calorimetric curve (Fig.3), the critical temperature A_s was determined and the temperature ranges of exothermic and endothermic processes were read off. From ~775 K up to ~850 K the transformation shows a slow course and has probably a diffusional character. In the temperature range 850÷950 K a considerable acceleration of the transformation takes place with a slight slowing-down at ~905 K. In the temperature range, transformation has martensitic character. At 950 K an abrupt slowing-down occurs which ends beyond the measuring range of the calorimeter used.

The calorimetric record corresponds partly with that obtained by means of the dilatometric method. In both the records A_s temperatures show only a slight difference while in the calometric record the diffusionless transformation starts at a temperature by ~75 K lower and stretches over a wider temperature range. These differences can be probably attributed to decomposition of the axial texture of martensite (specimens were sampled from wire) which mars the course of changes in elongation, originating from changes in the lattice structure. For this reason, the calorimetric method gives a more reliable record of the course of the reverse transformation.

As the electron microscopy examination shows, exotermic and endotermic effects accompanying the transformation are associated with the precipitation

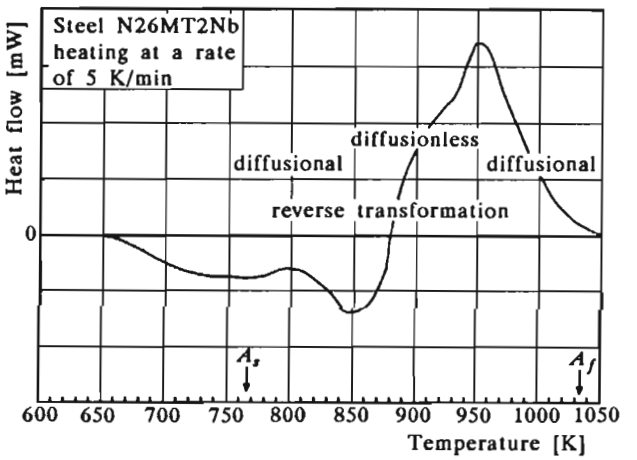

Fig. 3. Calorimetric curve of the reverse transformation with critical temperatures (approximate A_f) and the range of diffusionless or diffusional transformation marked therein

of the γ' phase in retained austenite and of the phase η in martensite. In the $\alpha' \rightarrow \gamma$ transformation a more important role is played by the ageing of martensite, which is responsible for the transformation slowing-down and for its diffusional character.

4.2. *X*-ray diffraction analysis

The peaks recorded in *X*-ray diffraction patterns originated exclusively from the martensite and austenite. Fig.4 shows, also, the content of martensite versus a tempering temperature. In the specimens quenched in liquid nitrogen the proportion of martensite was ~70%. With the rise in tempering temperature; i.e., with the progress in the $\alpha' \rightarrow \gamma$ transformation, the proportion of martensite decreased to ~45% at 925 K and to 5% at 1025 K, respectively.

4.3. Light microscopy

After quenching in liquid nitrogen, the steel microstructure was composed of large crystals of plate martensite with midribs, fine crystals of completely twinned thin-plate martensite and retained austenite (Fig.5a). Fig.5b shows the microstructure after tempering at 975 K, with a morphology similar to that

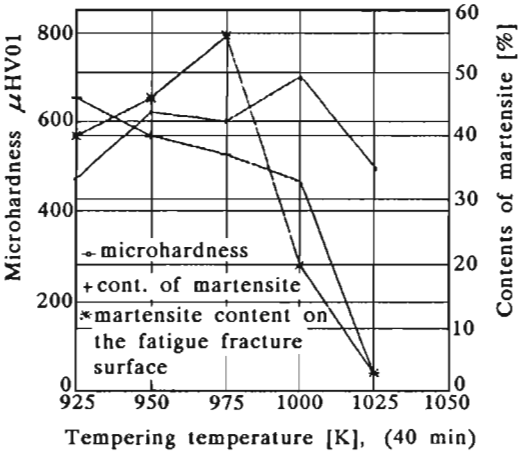

Fig. 4. Mean martensite content in the specimens microhardness of the two-phase structure and martensite content on fracture surfaces in specimens used for fracture toughness tests after tempering for 40 minutes at the indicated temperatures

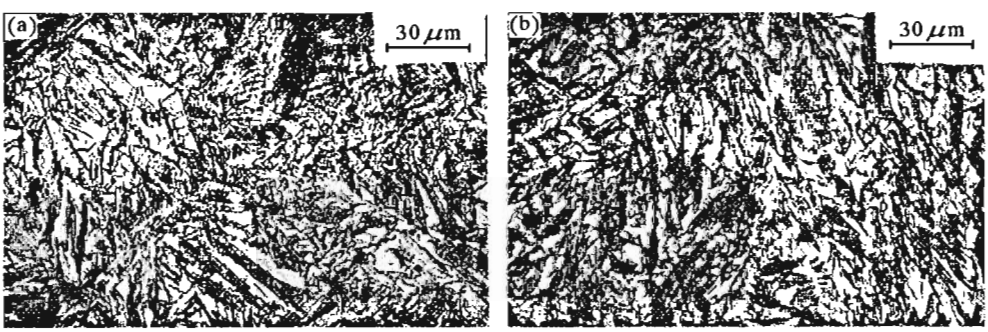

Fig. 5. Microstructure of Ni26MoTt2Nb steel: (a) – after cold treatment in liquid nitrogen; (b) – after tempering for 40 minutes at 975 K

of specimens tempered at other temperatures. Reverted austenite occured here in the form of ligth spots within the plates of martensite (Fig.5b).

4.4. Electron microscopy

Fig.6 shows the microstructure after quenching in liquid nitrogen. It is composed of plates of partly twinned martensite with midribs (Fig.6a), plates of completely twinned martensite, locally forming zigzags (Fig.6c) which are

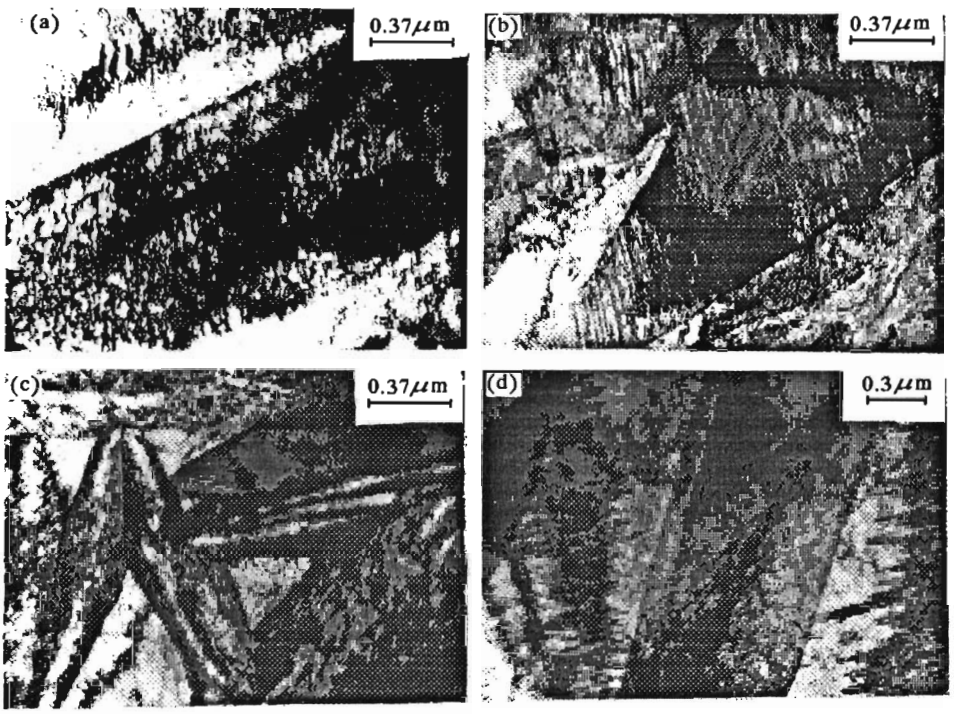

Fig. 6. Substructure after quench hardening in liquid nitrogen (a), (b) and (c) and after tempering for 40 minutes at 850 K (d)

characteristic of the athermal explosive kinetics, and retained austenite. In Fig.6d the plates of martensite after tempering for 40 minutes at 850 K are shown. They include no precipitates and do not show any sings of the reverse transformation.

In the parent cristals of martensite tempered at 925 K (Fig.7a) a tweed structure composed of martensite and reverted austenite as well as a structure consisting of alternately arranged plates of these phases was observed. Fig.7c presents the microstructure of a specimens tempered at 975 K, differing markedly from the previous one, with γ' precipitates of a spherical shape. The equiaxed form of grains suggests that a diffusional or massive transformation is here involved.

In the microstructure of specimens tempered at 1025 K (Fig.7d) austenite was predominant, but as a result of partial disapperance of the γ' phase an essential constituent of the structure has also become the η phase occuring in the form of chains at grain boundaries as well as within grains.

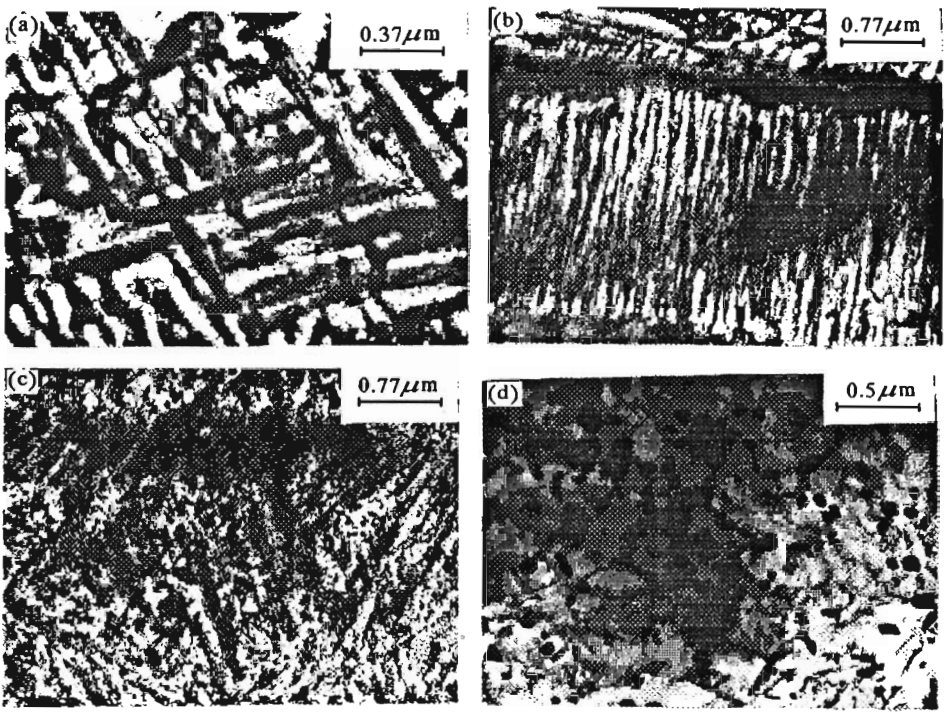

Fig. 7. Substructure after quench hardening in liquid nitrogen and after tempering at 925 K (a) and (b), 975 K (c) and 1025 K (d)

The identification of phases occuring in tempered specimens was performed by means of the electron diffraction method. As a basis for identification of the austenite form, the absence (reverted auste nite) or presence (retained austenite) of precipitates was adopted.

4.5. Tensile properties and fracture toughness

Fig.8 illustrates variation of the tensile strength R_m, the proof stress $R_{0.2}$ and the Young modulus E of the steel involved as a function of tempering temperature. The values involved differ markedly from those given in Table 1. Tensile strength and proof stress attained the highest values after tempering in the temperature range 925÷975 K and decreased rapidly with a further increase in temperature. Marked differences between the tensile strength and proof stress, reaching ~800 MPa, were observed. The Young modulus decreased

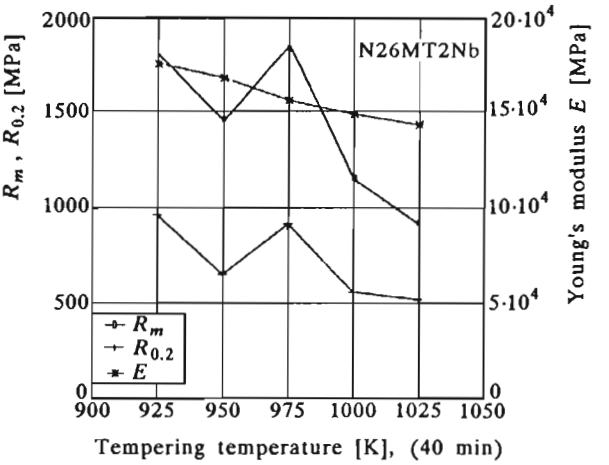

Fig. 8. Variation of R_m, $R_{0.2}$ and E during tempering

with the rise in tempering temperature, varying from 175 to 145 GPa. This was a result of the increase in proportion of reverted austenite.

The results of fracture toughness tests are shown in Fig. 9. After tempering at temperatures below 950 K, the value of the J_{Ic} remains at the same level ($\sim$30 kJ/m^2) after which it rises up to $\sim$58 kJ/m^2 at 975 K (this corresponds to $K_{Ic} = 102$ MPa m$^{1/2}$ attained by maraging steels of the Ni18Co9Mo5'type). After a decrease at 1000 K, this value rises anew up to 46 kJ/m^2. The fracture modulus T (Fig.9), expressed by two mathematical relationships, decreases in the temperature range 925$\div$975 K, whereupon it rises little more slowly above 1000 K. Thus an increase in fracture toughness is accompanied by a decrease in resistance to crack propagation.

The initial, low values of J_{Ic}, determined for specimens with a tweed structure, which have been tempered for 40 minutes, were considerably higher than those given in Table 1.

The maximum value of fracture toughness at a further increase in tensile strength, proof stress and microhardness, was observed after tempering at 975 K. This is a result of a decrease in the martensite content and of changes in its morphology, but-as the X-ray and magnetometric analyses have shown – the main responsibility for this is to be attributed to phase hardening of reverted austenite and to its transformation into martensite. The increase in martensite content on fracture surfaces was by more than 10-15% higher as compared with non-deformed regions (Fig.4). On tempering at 1000 K, precipitated particles of the η phase appeared at grain boundaries, which grew

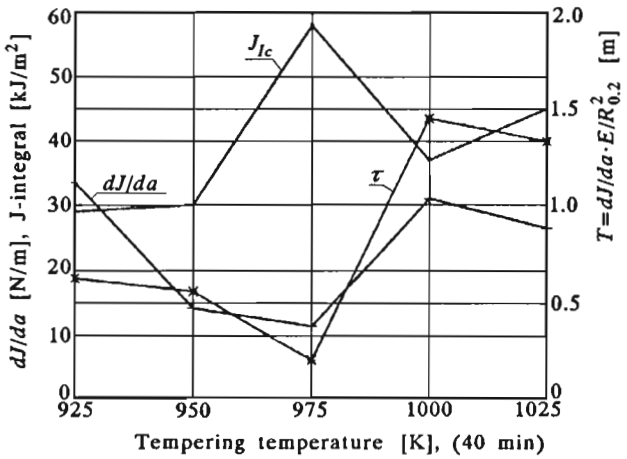

Fig. 9. Values of the J_{Ic} integral and of the fracture modulus T versus the tempering temperature

at the expense of γ' phase. This process along with a further increase in hardness, is probably responsible for the decrease in fracture touhgness. The disappearance of martensite at 1025 K and the rearrangement of the dislocation structure of austenite are the causes of a moderate increase in J_{Ic} in spite of the presence of large precipitated of the η phase.

Thus, the best set of strength properties and fracture toughness occured when the microstructure consisted of 38% martensite, ~30% retained austenite, and 32% reverted austenite which was transforming into martensite during crack formation.

4.6. Analysis of fracture surfaces

On fatigue fracture cracks (pre-cracks) as well as fracture surfaces in the region of crack propagation in specimens tempered at 850 K and at lower temperatures, characterized by relatively low values of J_{Ic} (~20 kJ/m^2), the localization of strains in macroscopic shear bands was observed as shown in Fig.10. This occured in the region of the fatigue fracture (Fig.10a,b) as well as in the zone of crack propagation (Fig.10c,d) giving rise to the secondary cracks or to cleavage fracture of martensite crystals situated before the crack front.

Fracture surfaces of specimens used in fracture toughness tests, tempered

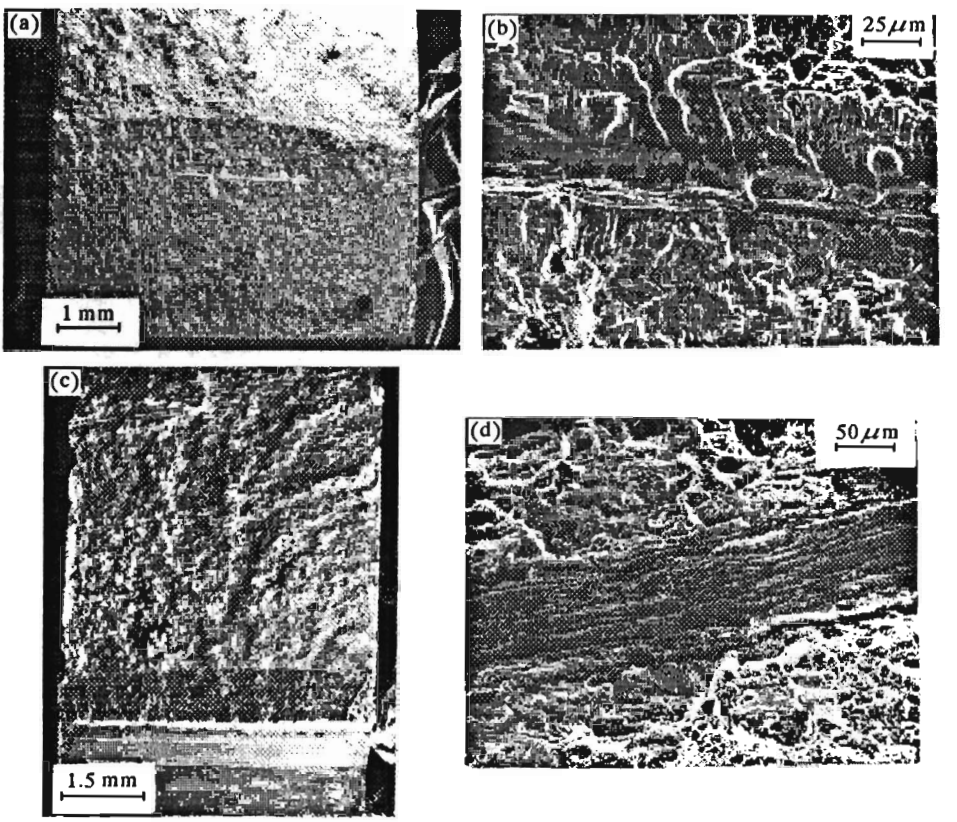

Fig. 10. Macroscopic shear bands on fracture surfaces of specimens used for determination of the J integral at 850 K ($J_{Ic} = 20\,\mathrm{kJ/m^2}$); (a) – in the fatigue fracture zone, (b) – in the region of crack propagation

at 925, 975 and 1025 K, are shown in Fig.11. Zones of fatigue fracture (pre-cracks) as well as those of the fracture formed at the stage of propagation, with increasing temperature show the following, characteristic behaviour.

In the fatigue zone, the most accentuated features of a transcrystalline cleavage fracture are found in specimens tempered at 975 K. In contrast to that, in specimens tempered at 925 K the occurence of these features was less marked. Smaller proportion of cleavage fracture along with a more developed surface in specimens tempered at 925 and 1025 K are accounted for by the presence of deformation martensite (after tempering at 925 K) or by incoherent precipitates at grain boundaries (after tempering at 1025 K).

In the zone of crack propagation, the largest proportion of an intercrystalline fracture was observed in specimens tempered at 975 K, while in those

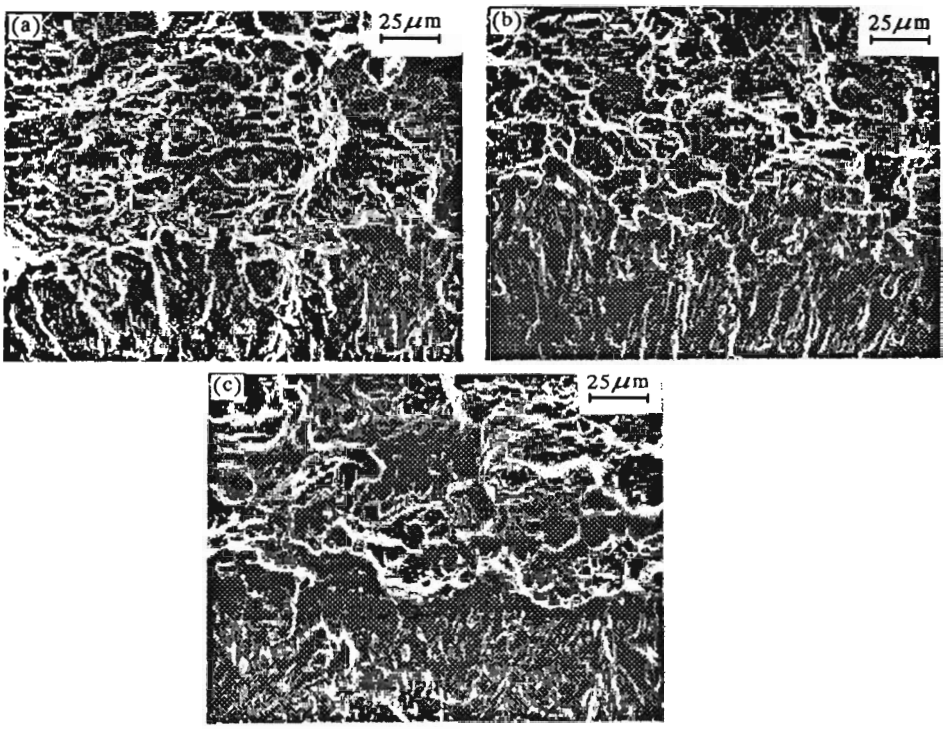

Fig. 11. Morphology of the fracture surfaces in the fatigue fracture zone (at the bottom) and in the crack propagation zone (at the top) in specimens used for the determination of J_{Ic} after tempering for 40 minutes at: (a) – 925 K, (b) – 975 K, (c) – 1025 K

tempered at 1025 K the proportion of a transcrystalline dimpled fracture prevailed.

Specimens tempered at 975 K showed most markedly accentuated features of a brittle fracture. This can be explained by the refinement of the microstructure resulting from the reverse transformation accompained by the phase hardening. This explanation also finds corroboration in the lowest fracture modulus value observed. After tempering at 1025 K, a dimpled fracture is formed in austenite containing incoherent precipitates. The fracture of specimens tempered at 925 K has a transcrystalline cleavage character and it originates from the cracking of martensite crystals along the cleavage planes containing precipitates.

5. Conclusions

Changes in tensile properties and fracture toughness after tempering are connected with changes in microstructure, resulting from by phase hardening and ageing. The results of this investigation confirm the following conclusions to be formulated:

- The most advantageous set of strehgth parametres and fracture toughness, comparable with that of maraging steels, is achieved after tempering under conditions in which reverted austenite is formed which, in turn, undergoes at room temperature a strain-induced martensitic transformation.

- An optimum fracture toughness of Ni26MoTi2Nb steel appears when the structure of this steel, after tempering for 40 minutes at 975 K, contains ~32% metastable reverted austenite, ~30% aged retained austenite and 38% retained martensite, respectively.

- The increase in fracture toughness is not adequate to the changes in morphology of the fracture surfaces observed. Especially conspicuous is a relatively small degree of development of the dimpled structure of the transcrystalline fracture.

- Small values of fracture toughness of Ni26MoTi2Nb steel along with clearly or relatively small tensile strength parameters and good or moderately good ductility are at insufficient metastability of austenite, responsible for the localization of plastic strains in macroscopic shear bands.

References

1. DAVIES R.G., MAGEE C.L., 1970, Austenite Ferromagnetism and Martensite Morphology, *Metall. Trans.*, **1**, 2927-2831

2. DAVIES R.G., MAGEE C.L., 1971, *Influence of Austenite and Martensite Strength on Martensite Morphology*, **2**, 1939-1947

3. DECKER R.F., 1963, in: *The Relation between Structure and Mechanical Properties of Metals (HMSO)*, London, 647-672

4. DEKHTYAR I.J. ET AL., 1984, Magnitnye svoystva zhelezoniklevykh splavov legirovannykh aluminiem i titanom posle otpuska v intervale $\alpha' \rightarrow \gamma$ prevrashchenya, *Metallofizika*, **6**, 2, 65-69

5. GERBERICH W.W., HEMMINGS P.C., MERZ M.D., ZACKAY V.F., 1968, Preliminary Toughness Results on TRIP Steel, *Trans. ASM,* **60**, 843-847

6. GORBACH V.G., ISMAYLOV E.A., MISHCHENKO S.S., 1984, Strukturnye raznovidnosti austenita, obrazujushegosya pri $\alpha' \rightarrow \gamma$ prevrashchenii v vysokoniklevykh splavakh, *Metallofizika,* **4**, 102-104

7. GORBACH V.G., ISMAYLOV E.A., ALEKHIN V.G., 1986, Prevrashchenye martensita v austenit v starejushchikh splavakh, *Izv. AN USSR Metally,* **2**, 122-126

8. GORBACH V.G., JELEŃKOWSKI J., FILIPIUK J., 1989, Microstructure and Mechanical Properties of Duplex Martensitic-Austenitic Fe-Ni-Ti Steels, *Mat. Sci. Tech.*, **1**, 5, 36-39

9. HORNBOGRN E., 1984, The Effect of Variables on Martensitic Transformation Temperatures, *Acta Metallurgica,* **33**, 595-601

10. JANA S., WAYMAN C.M., 1967, Martensite to FCC Reverse Transformation an Fe-Ni Alloy, *Trans. Met Soc. AIME,* 239, 1187-1193

11. JELEŃKOWSKI J., FILIPIUK J., 1991, Zmiany morfologii martenzytu w stopie N26MT2Nb wywołane cykliczną obróbką cieplną, *Inżynieria Materialowa,* 6(65), 145-151

12. KESSLER H., PITSCH W., 1967, On the Nature of the Martensite into Austenite Reverse Transformation, *Acta Metall.,* **15**, 401-405

13. KOKORIN V.V., 1987, *Martensitnye prevrashchenya v neodnorodnykh tvyordykh rastvorakh,* Iad. Naukova Dumka, Kiev

14. KORDONSKIY V.M., 1974, O mechanizmie "medllenogo" $\alpha' \rightarrow \gamma$ prevrashchenya v zhelezoniklevykh splavakh, *Fiz. Metal. Metalloved.,* 38, **2**, 366-375

15. KORDONSKIY V.M., 1974, Obratnoye $\alpha' \rightarrow \gamma$ prevrashchenye v zhelezo niklevykh splavakh, 38, **2**, 366-375

16. KULINCHEV G.P., PERKAS M.D., 1970, Issledovanye starenya austenita splavov na zhelezo-niklevoy osnovye, legirovannykh titanom i molibdenom, *Fiz. Metal. Metalloved.,* **29**, 5, 1018-1024

17. MALYSHEV K.A. ET AL., 1982, *Fazoviy naklop austenitnykh splavov na zhelezoniklevoy osnove,* Izd. Nauka Moskva

18. OLSON G.B., PARKS D.M., CHEN I-WEI, 1987, Mechanisms of Transformation Toughening, Final Report, Grant DOE/ER/45154-1, MIT, MASS

19. PICKERING F.B., 1978, *Physical Metallurgy and the Design of Steel,* Mat. Sc. Series, Applied Publishers LTD

20. RICHMAN R.H., BOLLING G.F., 1971, Stress, Deformation and Martensitic Transformation, *Metall. Trans.,* **2**, 2451-2462

21. SAGARADZE V.V., UVAROV A.U., 1989, *Uprochnenye austenitnykh staley,* Izd. Nauka, Moskva

22. SCHMIDT I., 1989, *Metastable Ferrous Austenite-Consequences on Fracture and Tribology,* Eds Hornbogen E., Jost N. in: *The Martensitic Transformation in Science and Technology,* Bochum

23. VERHOEVEN J.D., 1975, *Fundamentals of Physical Metallurgy,* 478

24. ZACKAY V.F., PARKER E.A., FHAR D., BUSCH R., 1967, The Enhancement of Ductility in High-Strength Steel, *Trans. ASM,* **60**, 252-259

Mikrostrkturalne uwarunkowania odporności na pękanie stali N26MT2Nb w stanie dwufazowym

Streszczenie

Badano wpływ 40 minutowego odpuszczania w temperaturowym zakresie $A_s \div A_f$, t.j. przemiany martenzytu w austenit, na mirostrukturę i odporność na pękanie stali N26MT2Nb o wyjściowej strukturze złożonej z ok. 70% martenzytu i ok.30% austenitu szczątkowego. W czasie odpuszczania stal ulegała starzeniu. Najwyższe wartości odporności na pękanie $-J_{Ic}$, czterokrotnie wyższe niż w stanie wyjściowym uzyskano po odpuszczaniu w temperaturze 975 K, bliskiej temperatury A_f. W wyniku odpuszczania nastąpił dwukrotny wzrost zawartości austenitu oraz ponad trzykrotny wzrost wytrzymałości na rozciąganie. Stwierdzony metodą rentgenograficzną ok. $10 \div 15\%$ wzrost zawartości martenzytu na przelomach próbek wygrzewanych w górnym zakresie temperaturowym przemiany $\alpha' \rightarrow \gamma$, w odniesieniu do miejsc nieodkształconych, świadczył o metastabilności austenitu nawrotu i korzystnym jego wpływie na odporność na pękanie.

Manuscript received August 25, 1994; accepted for print October 20, 1994